(10) Galin, M. *Macromolecules* **1977**, *10*, 1239.
(11) Ashworth, A. J.; Chien, C.-F.; Furio, D. L.; Hooker, D. M.; Kopečni, M. M.; Laub, R. J.; Price, G. J. *Macromolecules* **1984**, *17*, 1090.
(12) Haken, J. K. *J. Chromatogr.* **1984**, *300*, 1.
(13) Chien, C.-F.; Kopečni, M. M.; Laub, R. J. *HRC CC, J. High Resolut. Chromatogr. Chromatogr. Commun.* **1981**, *4*, 539.
(14) Chien, C.-F.; Furio, D. L.; Kopečni, M. M.; Laub, R. J. *HRC CC, J. High Resolut. Chromatogr. Chromatogr. Commun.* **1983**, *6*, 577.
(15) Rohrschneider, L. *J. Chromatogr. Sci.* **1970**, *8*, 105.
(16) Roth, M.; Novák, J. *J. Chromatogr.* **1982**, *234*, 337.
(17) Mandík, L.; Foksová, A.; Foltýn, J. *J. Appl. Polym. Sci.* **1979**, *24*, 395.
(18) After completing each run, replicate measurement at 30 °C was performed to check the significance of the bleeding of solvent from the column. With all the solvents studied, bleeding proved to be negligible.
(19) Cruickshank, A. J. B.; Windsor, M. L.; Young, C. L. *Proc. R. Soc. London, Ser. A* **1966**, *295*, 259.
(20) Everett, D. H. *Trans. Faraday Soc.* **1965**, *61*, 1637.
(21) Reid, R. C.; Prausnitz, J. M.; Sherwood, T. K. "The Properties of Gases and Liquids", 3rd ed.; McGraw-Hill: New York, 1977; Appendix A, pp 629–665.
(22) Spencer, C. F.; Adler, S. B. *J. Chem. Eng. Data* **1978**, *23*, 82.
(23) Hayden, J. G.; O'Connell, J. P. *Ind. Eng. Chem. Process Des. Dev.* **1975**, *14*, 209.
(24) Tsonopoulos, C. *AIChE J.* **1974**, *20*, 263.
(25) Dymond, J. H.; Smith, E. B. "The Virial Coefficients of Pure Gases and Mixtures. A Critical Compilation"; Clarendon Press: Oxford, England, 1980.
(26) Clarke, E. C. W.; Glew, D. N. *Trans. Faraday Soc.* **1966**, *62*, 539.
(27) Phillips, G. R.; Eyring, E. M. *Anal. Chem.* **1983**, *55*, 1134.
(28) Wičarová, O.; Novák, J.; Janák, J. *J. Chromatogr.* **1970**, *51*, 3.
(29) Laub, R. J.; Purnell, J. H.; Williams, P. S.; Harbison, M. W. P.; Martire, D. E. *J. Chromatogr.* **1978**, *155*, 233.
(30) Wičarová, O.; Novák, J.; Janák, J. *J. Chromatogr.* **1972**, *65*, 241.
(31) Neff, B.; Heintz, A.; Lichtenthaler, R. N. *Ber. Bunsen-Ges. Phys. Chem.* **1983**, *87*, 1165.
(32) Delmas, G.; Patterson, D.; Boehme, D. *Trans. Faraday Soc.* **1962**, *58*, 2116.
(33) Prausnitz, J. M. "Molecular Thermodynamics of Fluid-Phase Equilibria"; Prentice-Hall: Englewood Cliffs, NJ, 1969; p 293.
(34) Lichtenthaler, R. N.; Abrams, D. S.; Prausnitz, J. M. *Can. J. Chem.* **1973**, *51*, 3071.
(35) Heintz, A.; Neff, B.; Lichtenthaler, R. N. *Ber. Bunsen-Ges. Phys. Chem.* **1983**, *87*, 1169.
(36) Dolch, E.; Glaser, M.; Heintz, A.; Wagner, H.; Lichtenthaler, R. N. *Ber. Bunsen-Ges. Phys. Chem.* **1984**, *88*, 479.

Determination of Binodal Compositions of Poly(methyl methacrylate)/Sulfolane Solutions with Pulsed-NMR Techniques

Gerard T. Caneba and David S. Soong*

Department of Chemical Engineering, University of California, Berkeley, California 94720.
Received May 7, 1985

ABSTRACT: Binodal compositions of a poly(methyl methacrylate)/sulfolane system have been determined with spin–lattice relaxation of ^{13}C nuclei. Relaxation data obtained from inversion–recovery experiments are fitted with a modified Bloch equation to isolate distribution coefficients and spin–lattice relaxation time constants of ^{13}C nuclei of the polymer and solvent in polymer-rich and solvent-rich phases. Binodal compositions as a function of temperature are then computed from the overall composition of the starting binary polymer solution and the distribution coefficients.

Introduction

Current techniques for the determination of binodal compositions of polymer solutions include cloud point[1–4] and sedimentation[5] experiments. These methods have certain built-in disadvantages. Cloud point experiments require different samples for each point in the binodal curve; concentrated polymer samples take a very long time to equilibrate. As for sedimentation techniques, the main drawback is that phases in equilibrium need to be separated for subsequent analysis. Although all of the above-mentioned techniques have been successfully applied, they require a substantial amount of time and effort.

Pulsed-NMR techniques offer a potential solution to overcome the above difficulties in obtaining binodal compositions for polymer solutions. Experiments are done on samples in their mixed state; i.e., there is no need to separate the phases in equilibrium. Only one sample is needed to completely delineate the binodal curve if its overall composition is properly chosen. Magnetic field and/or radio-frequency perturbation are applied to alter the magnetic moments of certain nuclei in the mixed sample. When these perturbations are suddenly removed, the magnetic state of the affected nuclei will return to its unperturbed state with relaxation times that depend on the surrounding magnetic forces. If only two phases coexist, exactly two relaxation times can be resolved from the signal of a given type of nuclei. Certain perturbations or pulse sequences can be designed to maximize detection sensitivity by capitalizing on the differences in relaxation times for the same nuclei in different phases. This superposition in relaxation processes has been shown to be accurate for polymer–polymer systems.[6,7] In fact, the use of relaxation processes allows the analysis of a mixed system with overall compositions inside the phase envelope. Thus, compositions in the concentrated polymer phase are obtained from a system with a lower starting polymer concentration, greatly simplifying sample preparation.

In this work, we use the spin–lattice relaxation process to infer binodal compositions for a poly(methyl methacrylate)/sulfolane system. This is accomplished by using one sample for the entire procedure—one with an overall composition close to the critical or Θ point. This procedure is attempted in light of the successful use of spin–lattice and spin–spin relaxation by Kwei and his co-workers[6,7] for obtaining phase diagrams of polymer–polymer systems. We have hereby extended their methods to polymer/solvent systems, particularly in the case where the solvent is viscous enough to cause significant difficulties with conventional phase diagram determination technique. Reasonable results have been obtained for relaxation of ^{13}C nuclei in the polymer and solvent without magic-angle spinning.[8]

Theory

NMR spectroscopy[8] is based on the absorption of electromagnetic energy by nuclei at discrete frequencies or energy levels. Upon removal of the applied field, the nu-

0024-9297/86/2219-0369$01.50/0

clear spin system relaxes back to its original state by (a) interactions between nuclear spins, and (b) interactions between a nuclear spin and its surroundings. These two mechanisms are referred to as the spin–spin and spin–lattice relaxations, respectively.

The governing equation for the decay of the z-axis magnetization after a 180° pulse is the so-called Bloch equation[9]

$$M_z/M_0 = 1 - 2\exp(-t/T_1) \tag{1}$$

where M_z/M_0 is the relative magnetization along the direction of the equilibrium magnetization, M_0. T_1 is the spin–lattice relaxation time, and t is the time after removal of the field. If two phases coexist in the polymer/solvent system, a given type of nuclei will exhibit two different relaxation times. In this case, we have the modified version of the Bloch equation

$$M_z/M_0 = 1 - 2\phi^{(1)}\exp(-t/T_1^{(1)}) - 2\phi^{(2)}\exp(-t/T_1^{(2)}) \tag{2}$$

where $\phi^{(i)}$ is the atomic fraction of the given nuclei in phase i and $T_1^{(i)}$ is T_1 in phase i. In our experiments, the spin–lattice relaxation time constants are measured through the inversion–recovery pulse sequence[9] 180° pulse–relaxation time (τ)–90° pulse. By the application of Fourier transform of the decay curve after the 90° pulse, M_z/M_0 can be obtained as a function of τ. The ratio M_z/M_0 is then proportional to the peak height of a given type of nuclei. With such M_z/M_0 vs. τ data, we can determine $T_1^{(i)}$ and $\phi^{(1)}/\phi^{(2)}$ for the two components in the system by parameter estimation techniques. Finally, the compositions of phases in equilibrium follow the mass balance formulations

$$y^{(1)} = \frac{(1-z)(1+x_2)}{(1-z)(1+x_2) + x_2 z(1+1/x_1)}$$

$$y^{(2)} = \frac{(1-z)(1+x_2)}{(1-z)(1+x_2) + z(1+1/x_1)} \tag{3}$$

where $y^{(i)}$ is the segment fraction of the polymer in phase i (1 is sulfolane-rich, and 2 is PMMA-rich), x_j is the ratio $\phi_j^{(1)}/\phi_j^{(2)}$ for component j distributed over the two phases (also known as the distribution coefficient), and z is the overall segment fraction of polymer.

Experimental Section

Primary standard (MW = 54 000 and HI < 1.07, as confirmed by GPC results) atactic poly(methyl methacrylate) (PMMA), purchased from Pressure Chemical Co., was used in this study. Sulfolane (tetramethylene sulfone or 1,1-tetrahydrothiophene dioxide), purchased from Alfa Products, was used as the solvent. Appropriate amounts of PMMA and sulfolane were mixed at about 80 °C, a temperature above the upper critical solution temperature (UCST). The solution was transferred to a Wilmad 513-7PP NMR tube (10-mm o.d., 8.96-mm i.d.), flame-sealed, and kept in a convection oven at 90 °C for at least 4 weeks. Before a relaxation experiment, the temperature of the sample was quickly brought to the experimental temperature by immersion in a water bath. After a quenching period of at least 2 h, the sample was stored at the operating temperature for at least 1 day.

The spectrometer used to record ^{13}C spectra operates at a carbon nuclear resonance frequency of 45 MHz and has variable temperature control with temperature fluctuations less than ±0.3 °C. To obtain the overall composition of the polymer/solvent system, a series of one-pulse experiments was performed at 80 °C. Since our goal was to obtain signals for ^{13}C nuclei of the polymer and solvent, carbon–hydrogen decoupling was employed at all relevant frequencies to obtain a clean spectrum (broad-band decoupling). Locking of the magnetic field through a deuterium radiofrequency RF signal was not necessary because the field was stable enough to allow the use of a previously locked magnetic field setting from another sample. Since the natural abundance of ^{13}C is quite low, repeated experiments had to be performed to accumulate an acceptable signal-to-noise ratio. For a phase-separated system, inversion–recovery (spin–lattice relaxation) experiments utilized a composite 180° pulse,[10] followed by a relaxation period and a 90° pulse, which was shifted 180° (relative to the inversion pulse) on alternate scans.[11] This procedure helped to correct for sample and pulse field inhomogeneities as well as differences in the effective pulse field experienced by ^{13}C nuclei resonating at different frequencies.

From the resulting spectra obtained at different relaxation times, relative peak heights were measured for the relevant peaks. Relative peak height vs. relaxation time data were then fitted by the decay equation (eq 2) presented in the Theory section by using a modified Gauss–Newton optimization routine.[12] Finally, compositions of phases in equilibrium were computed from the parameters determined by the above curve-fitting procedure.

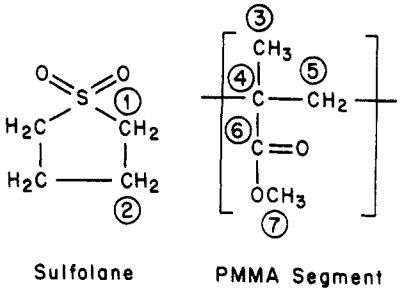

Figure 1. Structure formulas of sulfolane and PMMA showing the labels identifying carbon peaks in the spectrum shown in Figure 2.

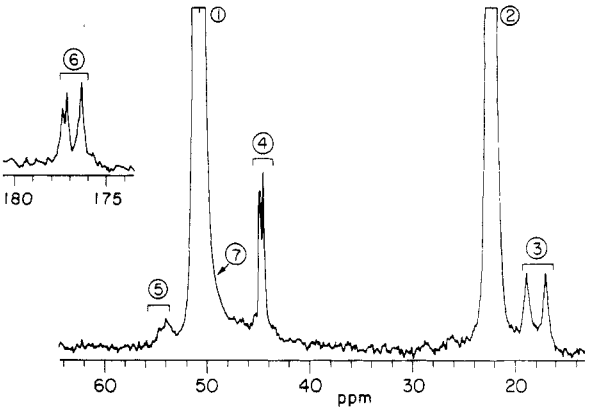

Figure 2. ^{13}C FTNMR spectrum of PMMA/sulfolane solution at 80 °C. A delay time of 10 s was used between scans. Total number of scans is 172.

Results and Discussion

From the molecular structures of PMMA and sulfolane (Figure 1), we identify peaks for ^{13}C atoms in the spectrum in Figure 2. For PMMA,[13] each repeat unit possesses an asymmetric center; stereochemical differences among randomly selected pairs of adjacent repeat units emerge in the resulting sample spectrum. If we take a given repeat unit, the two neighboring repeat units can be either isotactic (i) or syndiotactic (s) to the central unit. Such local tacticities are discernible in the ^{13}C spectrum (Figures 2 and 3). Figure 3 shows that the (ii) structure is about 62.5%. The remainder is primarily the (is) structure, and the (ss) structure is almost nonexistent. Calculation of areas under the peaks in Figure 2 revealed that the sample contains about 9.82 ± 0.05 wt % PMMA.

For data analysis of our inversion–recovery experiments, we focus on the 22-ppm solvent peak and the (ii) tertiary carbon polymer peak for peak-height measurements. At temperatures where phase separation occurs, influence of

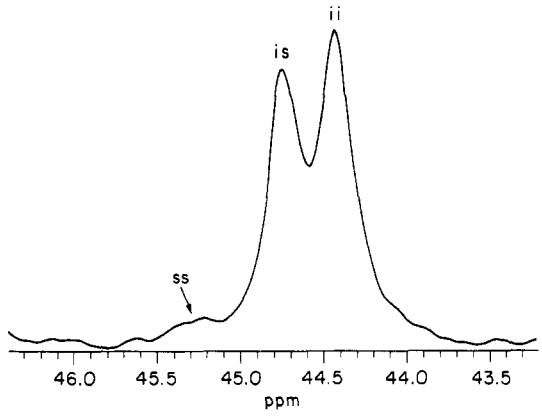

Figure 3. Expanded view of tertiary carbon PMMA peaks as seen in Figure 2, showing information about local stereochemistry of PMMA. Relative to a central PMMA repeat unit, the two adjacent repeat units are either isotactic (ii), syndiotactic (ss), or in mixed tacticities (is).

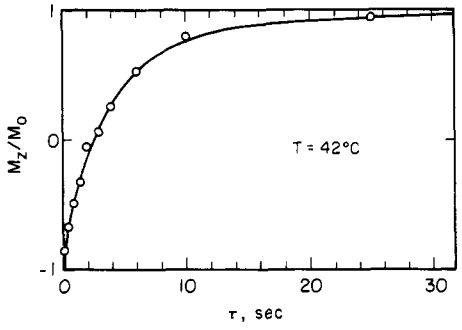

Figure 4. Relative magnetization as a function of the delay time (obtained from the peaks depicted in Figure 4) for the spin–lattice relaxation of the 22-ppm sulfolane peak at 42 °C.

the (is) peak on the (ii) peak is neglected. When the solidification point of the solvent is approached, the degree of overlap between the (is) and (ii) peaks is severe, and relaxation time results may become unreliable. The magnitude of this interference can be investigated by running the same experiments in a spectrometer with magic-angle spinning capabilities designed for solid samples.

The exact procedure is further illustrated for the solvent peak at 42 °C. Peak heights for different values of τ were measured (Figure 4) and made to fit the model equation (eq 2). Relaxation time constants of 0.128 and 5.03 s were obtained for this sulfolane peak in the polymer-rich and solvent-rich phase, respectively. In addition, the distribution coefficient (ratio of moles in the solvent-rich phase to that in the polymer-rich phase) is 6.66.

Figures 5 and 6 show results of all the calculations for sulfolane at different temperatures. Spin–lattice relaxation times for sulfolane are generally higher in the sulfolane-rich phase than in the PMMA-rich phase, and for both phases, they increase with temperature. These calculated relaxation time values for sulfolane in the sulfolane-rich phase are close to those reported for pure sulfolane.[14] Figure 6 shows that the distribution coefficient of sulfolane increases exponentially with decreasing temperature. As the temperature decreases, more sulfolane migrates to the sulfolane-rich phase, where the affinity with the surroundings is stronger. Although some scattering is evident, values read from such a linear fit of the semilogarithmic plot of x_1 vs. temperature can be used in subsequent model calculations.

The PMMA peak data can be similarly analyzed. Figure 7 indicates that the spin–lattice relaxation times in the

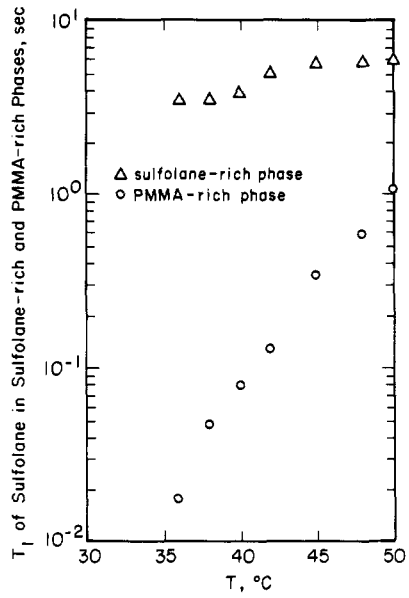

Figure 5. T_1 for the sulfolane peak at 22 ppm as a function of temperature in the sulfolane-rich and PMMA-rich phases.

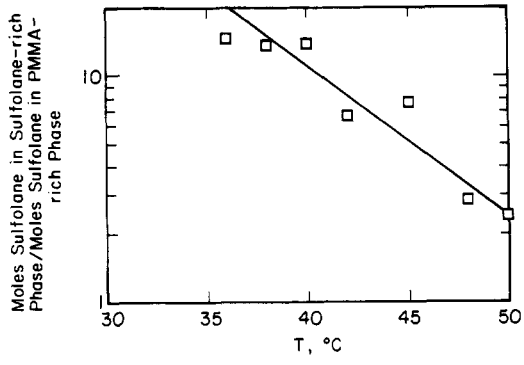

Figure 6. Distribution coefficient for sulfolane at different temperatures. The straight-line fit is determined by linear least-squares analysis of the semilogarithmic plot.

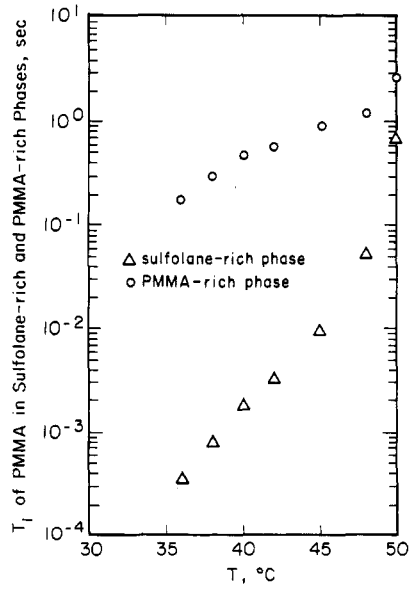

Figure 7. Averaged T_1 for the (ii) PMMA peak as a function of temperature in the sulfolane-rich phases.

PMMA-rich phase are generally greater than those in the sulfolane-rich phase and that for both phases they also increase with temperature. For the distribution coefficient of PMMA, Figure 8 shows that x_2 increases exponentially

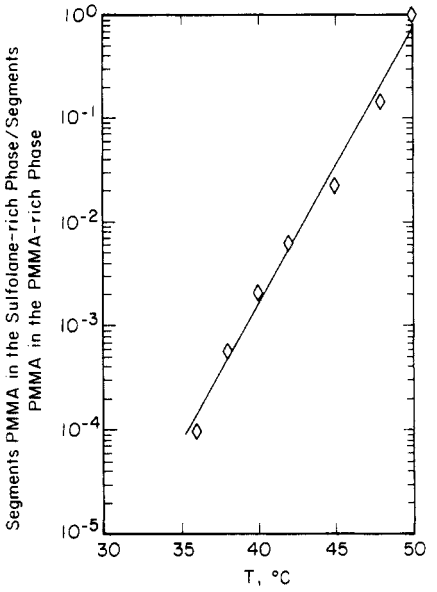

Figure 8. Distribution coefficient for PMMA at different temperatures. The straight-line fit is obtained from linear least-squares analysis of the semilogarithmic plot.

with temperature. This suggests that as the temperature decreases, more and more PMMA can be found in the PMMA-rich phase than in the sulfolane-rich phase. Again, for subsequent calculations, we use values read from a linear fit of this semilogarithmic plot.

Finally, the binodal curve can be determined by the simultaneous solution of the mass balance relations in eq 3. Figure 9 shows the resulting binodal curve. In view of the data scattering in Figures 6 and 8, as well as uncertainties in the determination of the overall composition of the mixture, errors in this curve are estimated to be ±0.07 in the PMMA-rich phase and ±0.03 in the sulfolane-rich phase. Furthermore, an extrapolation of the PMMA-rich phase to lower temperatures indicates that at the solidification point of the solvent (27 °C), the solvent concentration in the PMMA-rich phase is almost zero. This is a very encouraging result.

Explanations for trends of spin–lattice relaxation times are usually achieved through the so-called correlation time for random molecular motion, i.e., the average length of time a molecule remains in any given position before a collision causes it to change its state of motion.[9] Thus, the correlation time increases with a decrease in temperature and increase in viscosity of a liquid. Regardless of the detailed mechanism for spin–lattice relaxation, T_1 decreases with an increase in correlation time for small molecules. For macromolecules, T_1 can either increase or decrease with the correlation time.[9] Near the solidification point of a liquid, this situation is further complicated by the increasing significance of internal motions within molecules or polymer segments. More work is needed to explain the observed trends for spin–lattice relaxation times of sulfolane and PMMA. For the determination of the binodal curve, detailed understanding of these trends is not critical, as we are only interested in the ratios of components in different phases in equilibrium.

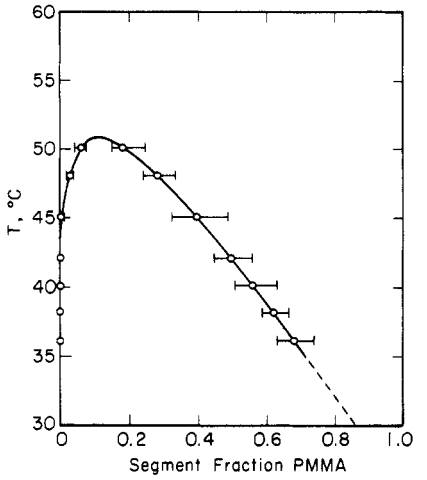

Figure 9. Binodal curve for the PMMA/sulfolane binary system determined from data presented in Figures 2, 7, and 9 along with the use of eq 3. Extrapolation of the polymer-rich phase to 27 °C, the solidification point of sulfolane, yields a value of $y^{(2)}$ close to 1.

Note that we have shown that even for a highly nonideal system, pulsed-NMR techniques offer an attractive alterative for the determination of binodal compositions of polymer solutions. Although we were not able to obtain relaxation data close to the solidification point of sulfolane, such a limitation is not inherent in the technique, nor is the technique demonstrated here limited to binary two-phase systems.

Acknowledgment. This work was supported by funds from the Polymer–Polymer Composites Program of the Center for Advanced Materials of Lawrence Berkeley Laboratory and the National Science Foundation through Grant CPE-8318681.

References and Notes

(1) Gavarot G.; Magat, M. *J. Chem. Phys.* **1949**, *46*, 355.
(2) Shultz, A. R.; Flory, P. J. *J. Am. Chem. Soc.* **1952**, *74*, 4760.
(3) Saeki, S.; Kuwahara, N.; Konno, S.; Kaneko, M. *Macromolecules* **1973**, *6*, 246.
(4) de Loos, T. W.; Poot, W.; Diepen, G. A. M. *Macromolecules* **1983**, *16*, 111.
(5) Chu, S. G.; Munk, P. *J. Polym. Sci., Polym. Phys. Ed.* **1977**, *15*, 1163.
(6) Kwei, T. K.; Nishi, T.; Roberts, R. F. *Macromolecules* **1974**, *7*, 667.
(7) Nishi, T.; Wang, T. T.; Kwei, T. K. *Macromolecules* **1975**, *8*, 227.
(8) Waugh, J. S.; Huber, L. M.; Haeberlen, U. *Phys. Rev. Lett.* **1968**, *20*, 180.
(9) Becker, E. D. "High Resolution NMR: Theory and Applications", 2nd ed.; Academic Press: New York, 1980.
(10) Freeman, R.; Kempsell, S. P.; Levitt, m. H. *J. Magn. Reson.* **1980**, *38*, 453.
(11) Cutnell, J. D.; Bleich, H. E.; Glasell, J. A. *J. Magn. Reson.* **1976**, *21*, 43.
(12) Gill, P. E.; Murray, W. *SIAM J. Numer. Anal.* **1978**, *15*, 977.
(13) Levy, G. C.; Lichter, R. L.; Nelson, G. L. "Carbon-13 Nuclear Magnetic Resonance Spectroscopy", 2nd ed.; Wiley: New York, 1980.
(14) Kydon, D. W.; Sharp, A. R.; Hale, M. E.; Watton, A. *J. Chem. Phys.* **1980**, *72*, 6153.